

## Prediction of a surface magnetic moment in $\alpha$ -uranium

N. Stojić,<sup>1,2</sup> J. W. Davenport,<sup>2</sup> M. Komelj,<sup>3</sup> and J. Glimm<sup>2,4</sup>

<sup>1</sup> *Department of Physics and Astronomy, Stony Brook University, Stony Brook, NY 11794-3381*

<sup>2</sup> *Center for Data Intensive Computing, Brookhaven National Laboratory, Building 463B, Upton, NY 11973-5751*

<sup>3</sup> *Jožef Stefan Institute, Jamova 39, SI-1000 Ljubljana, Slovenia and*

<sup>4</sup> *Department of Applied Mathematics and Statistics,  
Stony Brook University, Stony Brook, NY 11794-3600*

(Dated: November 20, 2018)

Recently, there has been an increased interest in first-principles calculations of the actinides as well as in finding the new materials which display surface magnetism. We predict the existence of a magnetic moment on the uranium (001) surface by performing density functional calculations for a slab geometry in the generalized gradient and local spin density approximations with included spin orbit coupling. The ferromagnetic phase is energetically favored for all geometries. The calculated total magnetic moment,  $0.65\mu_B$ , is stable on films of different thickness and it should be observable experimentally.

PACS numbers: 75.70.Ak, 75.70.Rf, 71.20.-b, 71.15.Mb

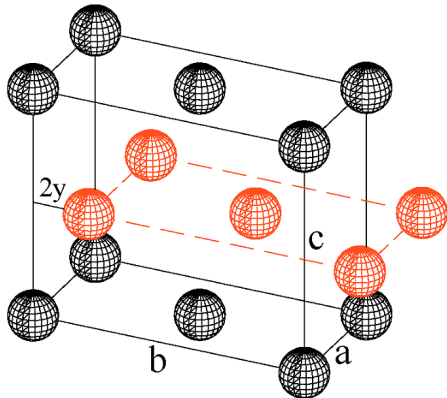
The beginnings of the field of surface magnetism can be traced back to the end of the 1960s with the claims of magnetic dead layers of some transition elements. In subsequent years it has been shown both experimentally and by first-principles calculations that Fe(001), Ni(001) and Cr(001) have considerable enhancement of magnetic moments at the surface with respect to the bulk value, [1]. As a rule one expects the tendency toward magnetism to be increased near metal surfaces, because of the narrowing of the density of states which yields a Stoner enhancement in the susceptibility. This lead to the search for surface magnetism in materials which are nonmagnetic in the bulk. There have been many attempts to find such materials (vanadium, for example), but most of them proved unsuccessful. To our knowledge the only experimentally clear case of a magnetic surface on a nonmagnetic metal is Rh(100), [2, 3]. In contrast, there are many examples of predicted transition metal monolayers on noble-metal substrates such as: Ti, V, Tc, Ru, and Rh on Ag or Au, [4].

Uranium would appear to be a possible candidate for surface magnetism since there is a rather large change in density of states from surface to bulk, as pointed out by Hao *et al.* [5]. Also, a comparatively modest expansion of the lattice leads to a spontaneous moment in the bulk which we have verified, [6]. In addition, it is near the transition (which occurs beyond plutonium) in which the 5f electrons become localized, [7]. We also note that many U alloys are magnetic, indicating the possible presence of a nearby magnetic instability. For example, URhAl [8] and UPtAl [9] are ferromagnetic with spin moments of order  $1\mu_B$ . In these structures the U atoms are in hexagonal planes (which include the transition element) and are separated by planes with no U.

We have explored the possibility for magnetism in uranium within the framework of the density functional theory (DFT). For uranium and the lighter actinides, DFT has been successful at predicting structural properties

[10, 11, 12]. For plutonium (and presumably for the heavier actinides) calculations which go beyond DFT (such as dynamical mean field theory) are required [13]. The calculations have been done using the orthorhombic structure ( $\alpha$ -uranium), Fig.1. This is the stable structure between 43K and 940K. At higher temperatures, it passes through tetragonal and then bcc structures before melting at 1408K. Below 43K the lattice undergoes a charge density wave (CDW) distortion [14]. The CDW distortions are only  $\approx 0.027 \text{ \AA}$ , [14], and were neglected. The orthorhombic structure may be viewed as a distorted bcc structure with the (001) plane similar to bcc (110) and with alternate (110) planes shifted along the  $b$  axis by  $(1/2 - 2y)b$ . A similar transformation was described by Axe *et al.* in [15]. The bcc structure would have  $y = 1/4$ ,  $a = a_{bcc}$ , and  $b = c = \sqrt{2}a_{bcc}$ . At the same volume  $a_{bcc} = 3.405 \text{ \AA}$ . The orthorhombic structure has  $a = 2.836 \text{ \AA}$ ,  $b = 5.866 \text{ \AA}$ ,  $c = 4.935 \text{ \AA}$ , and  $y = 0.1017$ , [16]. It belongs to the non-symmorphic space group Cmc. We confirmed previous calculations, [11], which show that this structure is lower in energy than bcc by 0.22 eV. We have also found that the bcc structure is mechanically unstable in the sense that the bcc energy is a relative maximum with respect to tetragonal distortions (a phonon calculation would lead to negative frequencies), [17]. For the calculations reported here we use the unrelaxed experimental geometry.

In this paper we solve the DFT equations using the WIEN2k, [18], implementation of the full potential linear augmented plane wave (FLAPW) method, [19], in a supercell geometry. To simulate a surface, we varied the length of the vacuum layer until no changes were noticed in energy and density of states and we kept it at 18 Bohr. Our free-standing monolayer calculations were done using 2 atoms per unit cell on a (001) surface, experimental lattice constants, 150 k points in the irreducible Brillouin zone and energy cutoff 12.5 Ry. For the film calculations (1 atom per surface cell), number of k-points varied from

FIG. 1:  $\alpha$ -uranium structure.

306 for the three-layer film to 153 for the seven-layer film. The muffin tin radius was kept fixed at 2.55 Bohr. For the exchange and correlation we used both the generalized gradient (GGA), [20], and the local spin density approximations (LSDA) for the monolayer and only GGA for the film calculations. In the actinides it is important to include several corrections to the usual scalar relativistic formulation of the FLAPW method. The spin orbit splitting of the 5f level in the isolated atom is 0.82 eV. This is comparable, though smaller than the f bandwidth which is of order 2 eV. Hence it is important to include spin orbit effects explicitly. This was done treating the spin orbit coupling in a second variation, [18]. Our bulk energy bands and density of states are in good agreement with fully relativistic results, [12]. In addition, the semicore 6s and 6p levels have bandwidths in the solid of order 2 eV so it is important to include them in the basis. In the Wien code they are treated by adding local orbitals at the appropriate energies, [21].

	GGA	GGA +SOC	LSDA	LSDA + SOC
FM	-0.333	-0.226	-0.241	-0.163
AFM	-0.206	-0.136	-0.141	-0.089

TABLE I: Calculated energy differences from the paramagnetic phase for the ferromagnetic (FM) and antiferromagnetic (AFM) state with and without spin-orbit coupling in GGA and LSDA for a monolayer in eV/atom.

We find that the surface does indeed support a magnetic moment. Our results for a monolayer, presented in Table I, demonstrate that the ferromagnetic (FM) phase is favored over antiferromagnetic (AFM) and paramagnetic (PM) phases. For the GGA with spin-orbit coupling (SOC) included, it lies 0.23 eV below the PM phase and 0.09 eV below the AFM phase. This result qualitatively does not depend on the exchange-correlation potential

	GGA	GGA+SOC	LSDA	LSDA + SOC
FM - sphere	2.42	2.11 (1.27)	2.13	1.97 (1.13)
FM - interstitial	0.85	0.74	0.71	0.62
FM - total per atom	3.27	2.01	2.84	1.75
AFM - total per atom	2.25	1.92 (0.79)	1.89	1.69 (0.59)

TABLE II: Calculated spin (spin + orbital) magnetic moments on spheres and in the interstitial region for the FM and AFM state with and without spin-orbit coupling in GGA and LSDA for a monolayer in units of  $\mu_B$ . Interstitial contribution is given per atom.

and inclusion of SOC. The direction of magnetization in the case with SOC is [001], perpendicular to the surface. The values of spin and total (orbital moment taken into account) magnetic moments on spheres and in the interstitial region for the FM and AFM phase are given in Table II. (Interstitial contributions come out as a consequence of the LAPW method's partitioning of space into atomic spheres and the interstitial region). We can see that the total moments per atom on the uranium monolayer are surprisingly large, 2.01 and 1.75  $\mu_B$  in GGA and LSDA, respectively. Total moment per atom is obtained by adding spin and orbital moments from a sphere to the spin interstitial moment. The orbital moments in the interstitial region vanish. We also compare the magnitude of the magnetic moments for the case without SOC. The moments are significantly larger in that case, similar to 4d and 5d (Ru, Rt, Pd, Os, Ir, Pt...) mono and double layers on Ag(001) and Au(001), [22].

Magnetic moments are similar in GGA and LSDA approximations. The influence of the type of the exchange and correlation approximation on the calculations of magnetic effects on surfaces is a subject of a discussion. For example, for chromium (001), [23], it was found that GGA tends to overestimate magnetic moments in bulk and at surface. However, the use of the LSDA for the description of a magnetic state also gave debatable results (bulk iron, for instance). All results presented further in this work have been obtained using the GGA.

The results for thick films are given in Table III. Since the calculated surface moment is stable upon the change in the slab thickness, we have performed calculations for up to seven layers. The constant value of the magnetic moment for the three cases is 0.65  $\mu_B$ . We show in Table III the spin and orbital moments in the outermost sphere and in the interstitial region for films of varying thickness. Interstitial moments are constant for the films of different thickness, from which we conclude that they are mostly at the surface. They are given per total calculational cell, so dividing them by two (two surfaces) and adding to the sum of spin and orbital moment, we get the total magnetic moment per atom. The moments diminish rapidly as a function of distance from the surface, so that, for example, for the five-layer film the total mo-

ments on the spheres are: 0.46, -0.03, and  $-0.04\mu_B$ . The orbital moments are relatively large. This is consistent with the findings for uranium compounds, [8]. In Table IV we present the energy differences from the PM to the FM phase for different films.

	1 layer	3 layers	5 layers	7 layers
spin moment	2.11	0.84	0.84	0.84
orbital moment	-0.38	-0.38	-0.38	-0.38
interstitial moment	0.74	0.39	0.38	0.38
total moment	2.01	0.66	0.65	0.65

TABLE III: Spin and orbital moments on spheres and in the interstitial region at the outermost layer for slabs of different thickness, with spin-orbit coupling, given in  $\mu_B$ . For 3 – 7 layers the total moment is taken to be spin + orbital + 1/2 interstitial.

1 layer	3 layers	5 layers	7 layers
-0.226	-0.011	-0.016	-0.020

TABLE IV: Energy differences from the paramagnetic state for different slab thickness geometries in eV/atom.

In order to justify our use of the unrelaxed experimental geometry in this work, we contracted the surface layer of a 5-layer slab. The energy minimum occurs at the contraction of 2.66%. We used the muffin tin radius of 2.35 Bohr and 72 k points in the irreducible Brillouin zone. The spin moment on a sphere of the relaxed structure was reduced slightly to  $0.65\mu_B$ .

We also calculated the surface energy using the unrelaxed geometry and including the SOC. It was found to be  $0.12 \text{ eV}/\text{\AA}^2$ . This is in a reasonable agreement with the only available experimental result of  $0.094 \text{ eV}/\text{\AA}^2$  [24]. Previous calculations of Kollar *et al.*, [25], gave  $0.16 \text{ eV}/\text{\AA}^2$ .

The existence of the surface magnetic moment can be ascribed to the reduction of the coordination number which causes narrowing and enhancing of the density of states at the Fermi level. This increase in the local density of states,  $n_{loc}(E_F)$ , results in fulfilling the Stoner criterion  $n_{loc}(E_F)I > 1$ , ( $I$  is the exchange integral). For reasonable values of  $I$  ( $\approx 0.2 - 0.4 \text{ eV}$ ), [27], this change in  $n_{loc}$  is sufficient to drive the system magnetic, as we observe. This can be seen from the density of states for a paramagnetic 7-layer film and bulk shown in Fig. 2. The local density of states at the Fermi level changes from 2.45 for bulk to 4.01 states/eV for the surface layer. It is even more pronounced for a monolayer, where PM local density of states at Fermi level reaches the value of 11.38 states/eV, Fig. 3. A similar effect of an emerging magnetic moment can be produced by a uniform expansion of the original lattice. For example, we have found that there is a magnetic moment of  $0.1\mu_B$  at the volume of

$26.5\text{\AA}^3$  ( $\approx 30\%$  increase). The moments increase with the further expansion.

In Fig.3 we show the spin-polarized density of states for a monolayer, which has a very sharp difference between spin up and down states. Figure 4 shows the spin-polarized density of states, for the surface layer of the 7-layer film.

Experimentally, the surface magnetism can be detected in a variety of ways including, for example, spin-polarized photoemission [2], linear or circular dichroism [3] and surface magneto-optic Kerr effect [28]. Given the size of our computed moments, these effects should be readily observable.

N. S. would like to thank E. Vescovo for many interesting and helpful discussions. Supported by US Department of Energy under Contract No. DE-AC02-98CH10886.

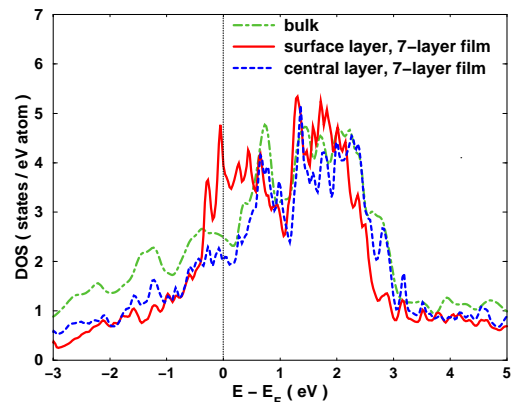


FIG. 2: Density of states for paramagnetic 7-layer film and bulk.

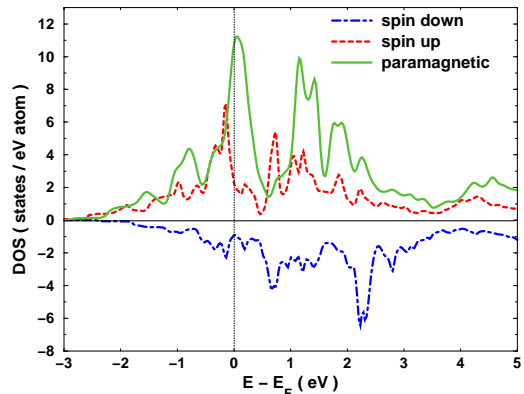


FIG. 3: Density of states for paramagnetic and magnetic monolayer.

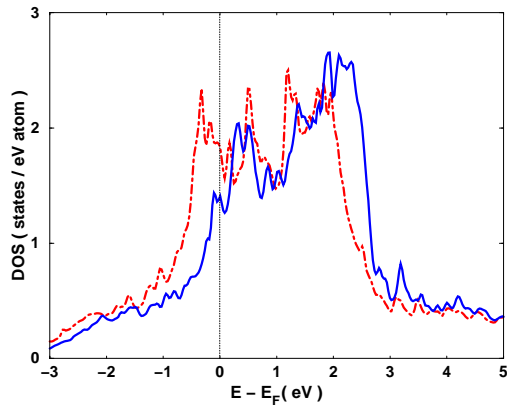


FIG. 4: Spin-polarized density of states for the outermost layer of the 7-layer film. The solid blue line represents the spin down density of states and the dot-dashed red line spin up density of states.

- 
- [1] See, for example: S. Ohnishi, A. J. Freeman, and M. Weinert, *Phys. Rev. B* **28**, 6741 (1983).  
 [2] S. C. Wu, K. Garrison, A. M. Begley, F. Jona, and P. D. Johnson, *Phys. Rev. B* **49**, 14081 (1994).  
 [3] A. Goldoni, A. Baraldi, G. Comelli, S. Lizzit, and G. Paolucci, *Phys. Rev. Lett.* **82**, 3156 (1999).  
 [4] See, for example: T. Asada, G. Bihlmayer, S. Handschuh, S. Heinze, Ph. Kurz, and S. Blügel, *J. Phys. Condens. Matter* **11** 9347 (1999).  
 [5] Y. G. Hao, O. Eriksson, G. W. Fernando, and B. R. Cooper, *Phys. Rev. B* **47**, 6680 (1993).  
 [6] A. Hjelm, O. Eriksson, and B. Johansson, *Phys. Rev. Lett.* **71**, 1459 (1993).  
 [7] S. S. Hecker, *MRS Bulletin* **26** 672 (2001).  
 [8] J. Kunes, P. Novak, M. Divis, and P. M. Oppeneer, *Phys. Rev. B* **63**, 205111 (2001).

- [9] A. V. Andreev, M. Divis, P. Javorsky, K. Prokes, V. Sechovsky, J. Kunes, and Y. Shiokawa, *Phys. Rev. B* **64**, 144408 (2001).  
 [10] M. D. Jones, J. C. Boettger, R. C. Albers, and D. J. Singh, *Phys. Rev. B* **61**, 4644 (2000).  
 [11] P. Söderlind, *Phys. Rev. B* **66**, 085113 (2002).  
 [12] H. Yamagami and A. Hasegawa, *J. Phys. Soc. Jpn.* **59**, 2426 (1990).  
 [13] S. Y. Savrasov, G. Kotliar, and E. Abrahams, *Nature* **410**, 793 (2001).  
 [14] J. C. Marmeggi, G. H. Lander, S. van Smaalen, T. Bruckel, and C. M. E. Zeyen, *Phys. Rev. B* **42**, 9365 (1990).  
 [15] J. D. Axe, G. Grubel, and G. H. Lander, *J. Alloys and Compounds* **213/214**, 262 (1994).  
 [16] C. S. Barrett, M. H. Mueller, and R. L. Hitterman, *Phys. Rev.* **129**, 625 (1963).  
 [17] N. Stojić, J. Davenport, and J. Glimm (unpublished).  
 [18] P. Blaha, K. Schwarz, G. Madsen, D. Kvasnicka and J. Luitz, *WIEN2k, An Augmented Plane Wave + Local Orbitals Program for Calculating Crystal Properties*, (Karlheinz Schwarz, Technical Universität Wien, Austria, 2001). ISBN 3-9501031-1-2.  
 [19] E. Wimmer, H. Krakauer, M. Weinert, and A. J. Freeman, *Phys. Rev. B* **24**, 864 (1981).  
 [20] J. P. Perdew, K. Burke, and M. Ernzerhof, *Phys. Rev. Lett.* **77**, 3865 (1996).  
 [21] G. K. H. Madsen, P. Blaha, K. Schwarz, E. Sjöstedt, and L. Nordström, *Phys. Rev. B* **64**, 195134 (2001).  
 [22] B. Újfalussy, L. Szunyogh, and P. Weinberger, *Phys. Rev. B*, **51**, 12836 (1995).  
 [23] G. Bihlmayer, T. Asada, and S. Blügel, *Phys. Rev. B*, **62**, R11937 (2000).  
 [24] *CRC Handbook of Chemistry and Physics*, (CRC Press, Boca Raton, 1992), 73<sup>rd</sup> edition, p.4-141.  
 [25] J. Kollar, L. Vitos, and H. L. Skriver, *Phys. Rev. B*, **49**, 11288 (1994).  
 [26] J. W. Ross and D. J. Lam, *Phys. Rev.*, **165**, 311 (1968).  
 [27] J. F. Janak, *Phys. Rev. B*, **16**, 255, (1977).  
 [28] Z. Q. Qiu and S. D. Bader, *J. Magn. Magn. Mat.*, **200**, 664 (1999).